ELSEVIER

Biophysical Chemistry 58 (1996) 109–116

Biophysical Chemistry

Electro-optics of membrane electroporation in diphenylhexatriene-doped lipid bilayer vesicles

S. Kakorin [a], S.P. Stoylov [b], E. Neumann [c,*]

[a] *Molecular Biophysics, Faculty of Physics, University of St.-Petersburg, St.-Petersburg, 198904, Russia*
[b] *Institute of Physical Chemistry, Bulgarian Academy of Sciences, Acad. G. Bonchev Str., Sofia, 1113, Bulgaria*
[c] *Physical and Biophysical Chemistry, Faculty of Chemistry, University of Bielefeld, P.O. Box 100131, D-33501 Bielefeld, Germany*

Received 15 February 1995; revised 23 March 1995; accepted 30 March 1995

Abstract

The electric (linear) dichroisms observed in the membrane electroporation of salt-filled lipid bilayer vesicles (diameter $\varnothing = 2a = 0.32$ μm; inside [NaCl] = 0.2 M) in isotonic aqueous 0.284 M sucrose–0.2 mM NaCl solution indicate orientation changes of the anisotropic light scattering centers (lipid head groups) and of the optical transition moments of the membrane-inserted probe 1,6-diphenyl-1,3,5-hexatriene (DPH). Both the turbidity dichroism and DPH absorbance dichroism show peculiar features: (1) at external electric fields $E \geq E_{sat}$ the time course of the dichroism shows a maximum value (reversal): $E_{sat} = 4.0$ (± 0.2) MV m^{-1}, $T = 293$ K (20°C), (2) this reversal value is independent of the field strength for $E \geq E_{sat}$, (3) the dichroism amplitudes exhibit a maximum value $E_{max} = 3.0$ (± 0.5) MV m^{-1}, (4) for the pulse duration of 10 μs there is one dominant visible normal mode, the relaxation rate increases up to $\tau^{-1} \approx 0.6 \times 10^6$ s^{-1} at E_{sat} and then decreases for $E > E_{sat}$. The data can be described in terms of local lipid phase transitions involving clusters L_n of n lipids in the pore edges according to the three-state scheme C $\rightleftharpoons$ HO $\rightleftharpoons$ HI, C being the closed bilayer state, HO the hydrophobic pore state and HI the hydrophilic or inverted pore state with rotated lipid and DPH molecules. At $E \geq E_{sat}$, further transitions HO $\rightleftharpoons$ HO* and HI $\rightleftharpoons$ HI* are rapidly coupled to the C $\rightleftharpoons$ HO transition, which is rate-limiting. The vesicle geometry conditions a $\cos\theta$ dependence of the local membrane field effects relative to the $\vec{E}$ direction and the data reflect $\cos\theta$ averages. The stationary induced transmembrane voltage $\Delta\varphi(\theta, \lambda_m) = -1.5aEf(\lambda_m)|\cos\theta|$ does not exceed the limiting value $\Delta\varphi_{sat} = -0.53$ V, corresponding to the field strength $E_{m,sat} = -\Delta\varphi_{sat}/d = 100$ MV m^{-1} (10^3 kV cm^{-1}), due to increasing membrane conductivity λ_m. At $E = E_{sat}$, $f(\lambda_m) = 0.55$, $\lambda_m = 0.11$ mS m^{-1}. The lipid cluster phase transition model yields an average pore radius of $\bar{r}_p = 0.35$ (± 0.05) nm of the assumed cylindrical pore of thickness $d = 5$ nm, suggesting an average cluster size of $\langle n \rangle = 12$ (± 2) lipids per pore edge. For $E > E_{sat}$, the total number of DPH molecules in pore states approaches a saturation value; the fraction of DPH molecules in HI pores is 12 (± 2)% and that in HO pores is 48 (± 2)%. The percentage of membrane area $P \approx (\lambda_m/\lambda_i) \times 100\%$ of conductive openings filled with the intravesicular medium of conductance $\lambda_i = 2.2$ S m^{-1} linearly increases from $P \approx 0\%$ ($E = 1.8$ MV m^{-1}) to $P = 0.017\%$ ($E = 8.5$ MV m^{-1}). Analogous estimations made by Kinosita et al. (1993) on the basis of fluorescence imaging data for sea urchin eggs give the same order of magnitude for P (0.02–0.2%). The increase in P with the field strength is collinear with the increase in concentration of HI and HI* states with the field strength, whereas the HO and HO* states exhibit a sigmoid field dependence. Therefore our data suggest that it is only the HI and HI* pore states which are conductive. It is noted that the various peculiar features of the dichroism data cannot be described by simple whole particle deformation.

* Corresponding author.

SSDI 0301-4622(95)00090-9

Keywords: Vesicles; Electroporation; Turbidity dichroism; Lipids; Membranes; Diphenylhexatriene

1. Introduction

Electric field pulses have traditionally been applied to probe ionic and dielectric properties of molecules and membranes and, recently, to manipulate biological cells and tissue. In particular, the membrane electroporation methods have gained increasing importance for cell biology, biotechnology and medicine [1]. The various applications include the direct (electrophoretic) transfer of genes (cell electrotransformation [2,3]) and other nucleic acids and of (ionic) proteins into the interior of cells and organelles, electrofusion to produce hybridoma cells, the electroinsertion of foreign glycoproteins into the membranes of blood organelles [4], transdermal drug delivery [5], and most recently the electrochemotherapy of skin tumors [6,7].

Electro-optic and conductometric relaxation spectrometric techniques provided evidence that the primary field effect on the dielectric membranes is ionic interfacial polarization resulting in large transmembrane electric potential differences $\Delta\varphi$ across the membrane thickness d. The large transmembrane field $E_m = -\Delta\varphi/d$ promotes water entrance [8] leading to lipid rearrangements in lipid bilayer vesicles [9,10]. In model membranes the data are consistent with the transient formation of hydrophobic (HO) and hydrophilic (HI) (inverted) pores, fluctuating in size and number and slowly resealing after pulse termination [11]. By applying the dip patch clamp technique it was shown that highly charged polyelectrolytes like DNA are electrophoretically drawn through electroporated membrane regions of many small pores; no large pores appear to be necessary [12]. The progress in the theoretical analysis provides the means to tackle the $\cos\theta$ dependence of the local field effects and yields further details such as the average pore size and the number of lipids in the pore edge.

2. Electro-optic key data

The primary electro-optic data of salt-filled lipid bilayer vesicles doped with the membrane probe 1,6-diphenyl-1,3,5-hexatriene (DPH), are the field-induced reduced absorbance changes $\Delta A^{\sigma}/A_0$ relative to the zero-field absorbance A_0, for the two light polarization modes $\sigma = 0°$ (parallel, $\Delta A^{\parallel}$) and $\sigma = 90°$ (perpendicular, $\Delta A^{\perp}$) relative to the direction of the external field vector $\vec{E}$. It can be shown that the difference of the modes measures the reduced linear dichroism, classically defined as

$$\frac{\Delta A^{-}}{A_0} = \frac{\Delta A^{\parallel} - \Delta A^{\perp}}{A_0} \qquad (1)$$

In addition to the DPH dichroism, the sum of the measured modes dominantly reflects changes in the immediate environment of the DPH probe molecule

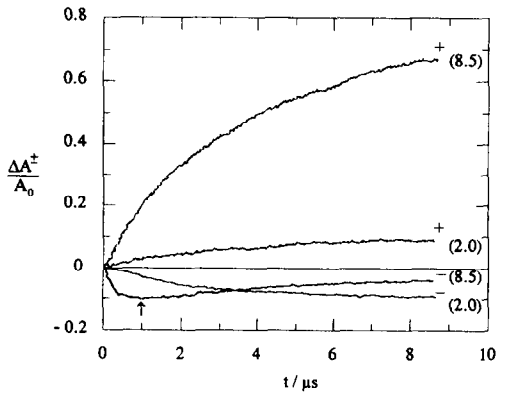

Fig. 1. The sum $\Delta A^{+}/A_0 = (\Delta A^{\parallel} + \Delta A^{\perp})/A_0$ (positive quadrant) and the difference (reduced dichroism) $\Delta A^{-}/A_0 = (\Delta A^{\parallel} - \Delta A^{\perp})/A_0$ (negative quadrant) of the relative absorbance changes at the parallel ($\sigma = \parallel$) and perpendicular ($\sigma = \perp$) light polarization modes ($\lambda = 365$ nm), respectively, as functions of time, at the two (extreme) field strengths $E = 2.0$ and $E = 8.5$ MV m^{-1}, respectively. Rectangular electric pulse of the field strength E and the pulse duration $t_p = 10$ μs (recorded up to $t = 8$ μs) at $T = 293$ K (20°C). Salt-filled unilamellar lipid vesicles doped with 1,6-diphenyl-1,3,5-hexatriene (DPH, $M_r = 232$), mean diameter $\varnothing = 320(\pm 80)$ nm, internal [NaCl] = 0.2 M, total lipid concentration [Lip$_t$] = 1.5 mM, [DPH$_t$] = 5 μM, vesicle density $\rho_v = 10^{12}$ ml^{-1}, suspended in isotonic 0.284 M sucrose–0.2 mM NaCl solution, pH 6.6. The zero-field DPH absorbance is $A_0 = OD_0(V,D) - OD_0(V) = 0.22$, as difference between the measured optical densities OD_0 of the doped vesicle (V,D) and non-doped vesicle (V) suspension. The arrow indicates the reversal time point for $E = 8.5$ MV m^{-1}.

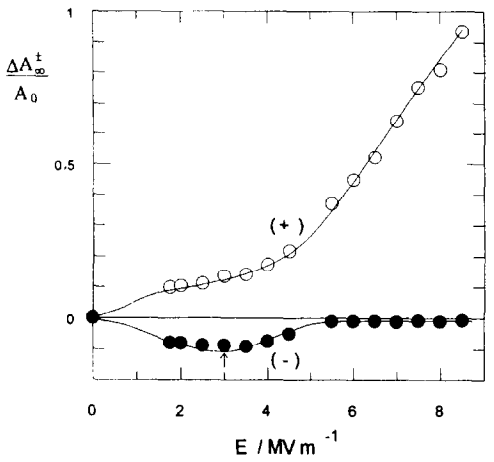

Fig. 2. The relaxation amplitudes of the sum $\Delta A_\infty^+ / A_0 = \Delta A^+(t \rightarrow \infty)/A_0$ (positive quadrant) and the difference $\Delta A_\infty^- / A_0 = \Delta A^-(t \rightarrow \infty)/A_0$ (negative quadrant) as functions of the external field strength E, respectively. (○) $\Delta A_\infty^+ / A_0$ and (●) $\Delta A_\infty^- / A_0$ were obtained from the $\Delta A^\sigma / A_0$ time dependencies for $t \rightarrow \infty$, $\sigma = \parallel, \perp$. Experimental conditions as in Fig. 1. The arrow indicates the maximum reduced dichroism value $|\Delta A^- / A_0| = -0.11$.

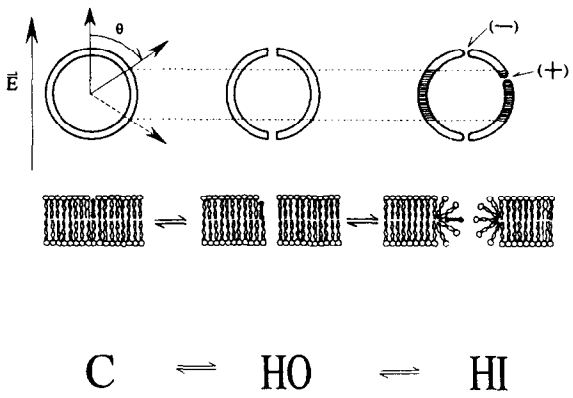

Fig. 3. Vesicle geometry, scheme for the molecular rearrangements of the lipids and the probe DPH in the pore edges and scheme for the lipid cluster phase transitions. In the HI pore edge the DPH molecules are taken along with the rotation of the lipid molecules. For the light polarization mode parallel to the direction of the electric field vector $\vec{E}$, the DPH rotation in the pole region turns the optical transition moment of the probe out of the favorable light absorption direction, causing a negative contribution to the absorbance dichroism ($\Delta A^- / A_0 < 0$). For the equatorial vesicle region ($54.7° < \theta < 125.3°$, shaded area), the same type of DPH movement turns the optical transition moment into the light absorption direction, leading to a positive contribution to the absorbance dichroism.

due to entrance of water and small ions into the lipid phase in the process of pore formation.

$$\frac{\Delta A^+}{A_0} = \frac{\Delta A^{\parallel} + \Delta A^{\perp}}{A_0} \qquad (2)$$

In Fig. 1 the time courses of the signals ΔA^- and ΔA^+ are shown for two (extreme) field strengths. The data indicate negative linear dichroism reflecting the dominance of the DPH molecules, which have changed their optical transition moments in the direction perpendicular to the direction of $\vec{E}$. Fig. 2 shows the field dependence of the amplitudes $\Delta A_\infty = \Delta A(t \rightarrow \infty)$ of the relaxation signals. Note that the reduced dichroism $|\Delta A_\infty^- / A_0|$ passes through a maximum value at $E_m = 3.0\ (\pm 0.5)$ MV m^{-1} (30 kV cm^{-1}).

3. Theory and data analysis

3.1. Normal mode parameters

The DPH relaxation data can be described in terms of local lipid phase transitions involving cooperative clusters L_n of n lipids in the pore edge. This physical-chemical "Ansatz" is cast in the global scheme (Fig. 3):

$$C \underset{k_{-1}}{\overset{k_1}{\rightleftarrows}} HO \overset{K_2}{\rightleftarrows} HI \qquad (3)$$

The lipid cluster phase transition from the closed bilayer state C to the hydrophobic pore HO turns out to be rate-limiting for the rapid HO ⇄ HI equilibration.

Normal mode analysis yields the relaxation rate

$$\frac{1}{\tau} = k_1 + k_{-1}\frac{1}{1+K_2} = k_{-1}\left(K_1 + \frac{1}{1+K_2}\right) \qquad (4)$$

where $K_1 = [HO]/[C] = k_1/k_{-1}$ is the equilibrium constant of the first step, k_1 and k_{-1} are the rate constants and $K_2 = [HI]/[HO]$ is the equilibrium constant of the second step.

For higher field strengths $E \geq 4.0\ (\pm 0.2)$ MV m^{-1} two additional, optically different states HO*

and HI* are required to describe the data. The lipid cluster phase transition HO ⇄ HO* with $K_{HO} = [HO^*]/[HO]$ and HI ⇄ HI* with $K_{HI} = [HI^*]/[HI]$ are rapidly coupled to the cascade in scheme 3. For this case the quantity K_2 in Eq. 4 is replaced by the term $\bar{K}_2 = K_2 + K_{HO}(1 + K_2^*)$, where $K_2^* = [HI^*]/[HO^*] = K_2 K_{HI}/K_{HO}$.

Since the interfacial ionic polarization (Maxwell–Wagner) is very fast [1], i.e. $\tau_{pol} \ll \tau$, the integral chemical relaxation of the states described by $[HO] + [HO^*] = [HO](1 + K_{HO})$, which are dominantly covered by the ΔA^+ time courses, is given by

$$[HO] = [HO]_\infty\left(1 - e^{-\frac{1}{\tau}t}\right) \tag{5}$$

where $[HO]_\infty$ denotes the amplitude.

The time course of the reduced dichroism signals $\Delta A^-/A_0$ basically reflects the concentrations $[HI] + [HI^*] = [HI](1 + K_{HI})$ and is described by

$$[HI] = [HI]_\infty\left(1 - e^{-\frac{1}{\tau}t}\right) \tag{6}$$

At field strength $E > 4$ MV m^{-1} the initial larger increase in the dichroism signal ΔA^- observed within the first 6 μs is additional to the lipid cluster phase transitions covered by the reaction scheme 3 and the transitions HO ⇄ HO* and HI ⇄ HI*. The additional contribution is transient and is described by the direct lipid cluster phase transition C(⇄ HO*) ⇄ HI_Q^* with $K_Q = [HI_Q^*]/[C] = k_Q/k_{-Q}$; this transition only marginally contributes to the stationary values ΔA_∞^+ and ΔA_∞^-. The formal description includes the transient contribution in the quantity $\bar{K}_2$ by

$$\bar{K}_2 = K_2 + K_{HO}\left[1 + K_2^*\left(1 + K_{HI}^Q\right)\right] \tag{7}$$

where

$$K_{HI}^Q = \frac{[HI_Q^*(t, \theta, \lambda_m)]}{[HI^*]}$$

The minimum state reaction scheme necessary to describe all the observed relaxation is presented in scheme 8:

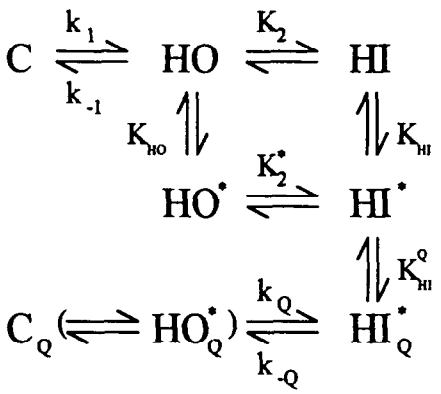

(8)

3.2. Vesicle geometry and dichroism

The lipid cluster phase transitions HO ⇄ HI, HO* ⇄ HI* and C(⇄ HO*) ⇄ HI_Q^* describe the turning of the lipid molecules from the bilayer conformation with the fatty acid tails of the lipids parallel to, toward a position perpendicular to the membrane normal. It appears that, because of K_2, K_2^* being independent of E, the membrane probe DPH is taken along with the turning lipids such that the optical transition moment of DPH in the HI, HI*, HI_Q^* states is perpendicular to the membrane normal. If the lipid cluster phase transitions occur in the pole cap regions (Fig. 3), it leads to negative dichroism. However, if the same type of transition occurs in the equatorial region, it yields a positive contribution to the absorbance dichroism. Due to the vesicle geometry the actual membrane field is $E_m \approx E|\cos\theta|$. Therefore, when the field strength E is increased, the electropore formation is spread from the pole caps to the equatorial region. At $\theta \geq 54.7°$ the positive contributions begin to reduce the overall negative absorbance dichroism. This particular feature is the origin of the maxima or reversal points observed in the time course of the dichroism signal and in the field dependence of the amplitude (Figs. 1 and 2). At $E > E_{sat}$ the transient occurrence of the lipid cluster phase transition C(⇄ HO*) ⇄ HI_Q^*, even though it is restricted to the pole cap region, can also be the origin of the reversal point in the time course of the dichroism signal, but not of that in the field dependence of the stationary amplitude value.

The electro-optic analysis specifies the observed signal $\Delta A^{\sigma} = \Delta A^{\sigma}_{OR} + \Delta A^{\sigma}_{CH}$ as the sum of a purely orientation term ΔA^{σ}_{OR} and a chemical term ΔA^{σ}_{CH} [13]. It can be shown that in contrast to the free orientation of chromophores in an isotropic environment, where the purely orientational contributions follow the relationship $\Delta A^{\parallel}_{OR} = -2\Delta A^{\perp}_{OR}$, the vesicle geometry and the HO ⇄ HI transition model leads to

$$\Delta A^{\parallel}_{OR} = -\Delta A^{\perp}_{OR} \tag{9}$$

The magic angle σ^* (where $A^{\sigma^*}_{OR} = 0$) of the HI pore model is 45° (and not 54.7°).

3.3. Transmembrane voltage and actual field

The electro-optic data confirm that the primary field effect on the vesicle suspension is the ionic interfacial polarization. The spherical geometry of a vesicle is the reason for the cos θ dependence of the induced transmembrane potential difference $\Delta\varphi$ in the direction of the external field strength vector $\vec{E}$. The stationary value is given by:

$$\Delta\varphi(\theta, \lambda_m) = -\frac{3}{2} aEf(\theta, \lambda_m)|\cos\theta| \tag{10}$$

where $a = \varnothing/2$ is the radius of the vesicle. The conductivity function $f(\theta, \lambda_m)$ can be expressed as [1]

$$f(\theta, \lambda_m) = \frac{1}{1 + \lambda_m(\theta)(2 + \lambda_i/\lambda_o)/(2\lambda_i d/a)} \tag{11}$$

where λ_m, λ_i, λ_o are the conductivities of the membrane, vesicle interior and the outside suspension, respectively.

The actual field driving the lipid cluster phase transition cascade is always directed along the membrane normal and its value is given by

$$E_m(\theta, \lambda_m) = -\Delta\varphi(\theta, \lambda_m)/d \tag{12}$$

where $d = 5$ nm is the average thickness of the bilayer (or the pore). Because $\vec{E}_m$ and $\vec{E}$ are related by $E_m \approx E|\cos\theta|$, *all measured field dependencies reflect* cos θ *averages.*

3.4. Field dependence of equilibrium constants

Analogous to the analysis by Abidor et al. [8] we may describe the field-induced membrane polarization changes in terms of a polarization difference

$$\Delta P = \varepsilon_0(\varepsilon_w - \varepsilon_L) E_m \tag{13}$$

where ε_0 is the vacuum permittivity, $\varepsilon_w \approx 80$ and $\varepsilon_w \approx 2$ are the dielectric constants of water and of lipids, respectively.

The cooperative transition of a lipid cluster L_n to form a pore with n lipid molecules in the pore edge is thermodynamically described by a (molar) phase transition dipole moment:

$$\Delta M = V_p N_A \Delta P \tag{14}$$

where N_A is the Avogadro constant and $V_p = \pi r_p^2 d$ is the aqueous pore volume of the assumed cylindrical pore. The analysis yields an average pore diameter

$$\bar{r}_p = \langle r_p^2 \rangle^{1/2} = \left(\langle V_p \rangle/(\pi d)\right)^{1/2}$$

The electric field dependence of the equilibrium constant of a dipolar equilibrium is generally described by

$$K(E) = K(0)e^{X} \tag{15}$$

where the field exponent X is given within the integration boundaries $E = 0$ and E by [14]

$$X = \frac{\int_0^E \Delta M \, dE}{RT} \tag{16}$$

Because of the special geometry and the interfacial polarization, the acting field is $E_m(\theta, \lambda_m)$ such that

$$X(\theta, \lambda_m) = \frac{V_p \varepsilon_0(\varepsilon_w - \varepsilon_L) E_m^2}{2k_B T} \cos^2\theta = w(E)\cos^2\theta \tag{17}$$

Applied to K_1 we obtain

$$K_1(\theta, E) = K_1(0)\exp\left[w_1(E)\cos^2\theta\right] \tag{18}$$

where $K_1(0)$ is K_1 at $E = 0$ and the field factor is given by

$$w_1(E) = \frac{9\pi\varepsilon_0 a^2(\varepsilon_w - \varepsilon_L)\bar{r}_p^2}{8k_B T d} f^2(\bar{\lambda}_m) E^2 \qquad (19)$$

The angular average of the membrane conductivity $\bar{\lambda}_m$ in $f^2(\bar{\lambda}_m)$ is expressed as:

$$\bar{\lambda}_m = \frac{1}{2}\int_0^{\pi} \lambda_m(\theta) \sin\theta \, d\theta \qquad (20)$$

The $\cos\theta$ average of the relaxation rate and of the amplitudes is obtained from, respectively:

$$\frac{1}{\tau} = \frac{\int_0^{t_p}\int_0^{\pi} [HO]_t^{\theta} \tau(\theta)^{-1} \sin\theta \, d\theta \, dt}{\int_0^{t_p}\int_0^{\pi} [HO]_t^{\theta} \sin\theta \, d\theta \, dt} \qquad (21)$$

$$[HO]_{\infty} = \frac{1}{4}\int_0^{\pi} [HO]_{\infty}^{\theta}(1 + \cos^2\theta)\sin\theta \, d\theta \qquad (22)$$

In Fig. 4 the $\cos\theta$ averaged relaxation rate τ^{-1} (Eq. 21) is presented as a function of field strength E. In contrast to the relaxation rate τ^{-1} ($\theta \approx 0$) for the lipid cluster phase transition cascade in the pole cap region (Fig. 4, dashed line), τ^{-1} does not approach a saturation value at $E > 4$ MV m^{-1} (see further details in the caption to Fig. 4).

Substitution of the Eqs. 5 and 22 for the HO states into $\Delta A^+ = (\varepsilon_{HO} - \varepsilon_C)[HO](1 + K_{HO})l$ (Lambert–Beer law), where l is the optical path length, yields the approximation

$$\frac{\Delta A^+}{A_0} \approx \frac{\Delta A_{\infty}^+}{A_0}\left(1 - e^{-\frac{1}{\tau}t}\right) \qquad (23)$$

where $\Delta A_{\infty}^+/A_0 = 3\beta_{HO}[HO]_{\infty}(1 + K_{HO})/[C_0]$, from which τ^{-1} can be evaluated.

The term $\beta = (\varepsilon_{HO} - \varepsilon_C)/\varepsilon_C$ includes the absorbance coefficients for the HO state and C state at $E = 0$; $[C_0]$ represents the total content of DPH probes in all membrane states. The exact expression contains rather complicated integration over the angle θ.

The derivation of corresponding expressions for the dichroism signal $\Delta A^-/A_0$ in terms of the $\cos\theta$ averages of the HI states, must take into account the different signs of the absorbance changes on the pole caps ($\theta \leq 54.7°$; $125.3° \leq \theta$) and in the equatorial region ($54.7° < \theta < 125.3°$) of the vesicle, respectively.

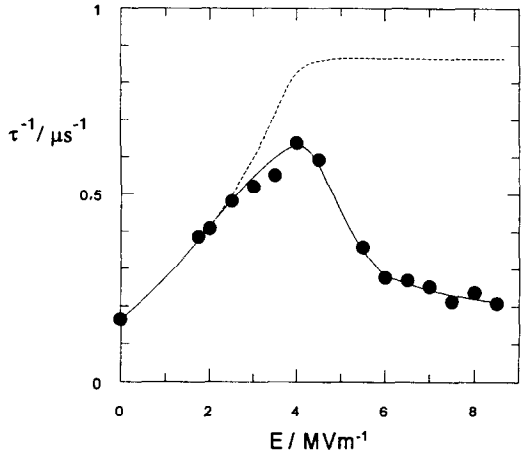

Fig. 4. The relaxation rata τ^{-1} ($\cos\theta$ average) of the normal mode relaxation (Eq. 21) as a function of the external field strength E. In addition, the dashed line indicates the relaxation rates τ^{-1} ($\theta \approx 0$) for the lipid cluster phase transition cascade in the pole cap region. The decrease in τ^{-1} at $E > 4$ MV m^{-1} reflects the contributions of the equatorial regions to the total absorbance; these contributions become increasingly larger. Note that the surface increment $\Delta S \approx \sin\theta\Delta\theta$ of a given $\Delta\theta$ increment is greater for the equatorial region than in the pole caps. However, the transmembrane field in the equatorial regions is lower and thus the reaction rates are smaller than in the pole cap regions.

4. Results and discussion

It is remarkable that, $E \leq 4$ MV m^{-1}, the rapid kinetics of the membrane electroporation in the time range $0 \leq t \leq 10$ μs can be consistently described by only one normal relaxation mode. The peculiar features of maxima in the time courses and in field dependencies are solely rationalized in terms of the $\cos\theta$ dependence of the actual membrane field strength $E_m \approx E|\cos\theta|$ ($0 \leq \theta \leq \pi$).

The fitting of the experimental curves $\Delta A^{\pm}/A_0$ (Fig. 1) and $\Delta A_{\infty}^{\pm}/A_0$ (Fig. 2) with the analytical expressions primary yields the field factor $w_1(E)$ associated with $K_1(E)$ and the absorbance factor $\beta(E)$. In Fig. 5 it is seen that $w_1(E)$ reaches a saturation value at $E_{sat} = 4.0(\pm 0.2)$ MV m^{-1}. The data are consistently described if, for $E \leq 1.8(\pm 0.2)$

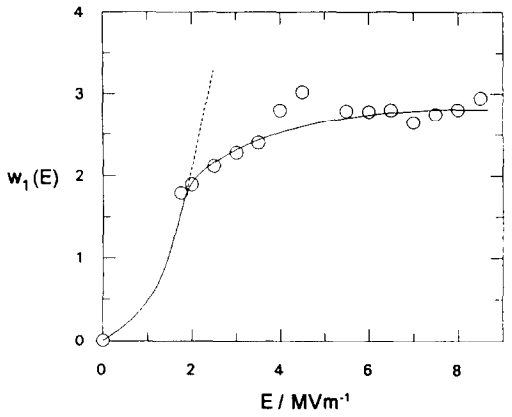

Fig. 5. The field factor $w_1(E)$ associated with the equilibrium constants $K_1(\theta,E) = K_1(0)\exp[w_1(E)\cos^2\theta]$ as a function of the field strength. The field factor contains the conductivity function $f(\bar{\lambda}_m)$, see Eq. 19 of the text. For $E < 2$ MV m^{-1}, $f(\bar{\lambda}_m) \approx 1$ corresponding to $\lambda_m \approx 0$.

MV m^{-1}, we use the physically plausible approximation that $\lambda_m \approx 0$, thus $f(\lambda_m) \approx 1$. Above this field strength, λ_m increases approximately linearly with E concomitant with the nearly linear increase in the amplitude $[HI]_\infty(1 + K_{HI})$, representing the enlargement of the concentration of conductive pores.

As a consequence of the increasing membrane conductivity, the transmembrane voltage reaches a saturation value $\Delta\varphi_{sat} = -0.53$ V, which is not exceeded even if $E > E_{sat}$. Corresponding to $\Delta\varphi_{sat}$ we obtain the limiting values of the actual membrane field $E_{m,sat} = -\Delta\varphi_{sat}/d = 100$ MV m^{-1} (or 10^3 kV cm^{-1}), $\lambda_m(E_{sat}) = 0.11$ mS m^{-1} and $f(\bar{\lambda}_m) = 0.55$, respectively, with $\lambda_i \approx 2$ S m^{-1} (due to [NaCl] = 0.2 M) and $\lambda_0 = 2.2$ mS m^{-1} (due to [NaCl] = 0.2 mM), $T = 293$ K (20°C).

Because of the saturation value of E_m, the field factor $w_1(E)$ and thus the equilibrium constant $K_1(\theta, E)$ in a given angular region of the vesicle membrane (Fig. 3) reaches a limiting value. $K_2 = 0.33$ and $K_2^* = 0.27$ turn out to be independent of E, classifying the HO $\rightleftarrows$ HI, HO* $\rightleftarrows$ HI* lipid cluster phase transitions as passive equilibrations coupled to the rate-limiting step C $\rightleftarrows$ HO. The field-dependent process should be primarily the entering of the (higher polarizable) water replacing the lipids during pore formation. Therefore, the field dependence of $K_1 = k_1/k_{-1}$ primarily resides in the rate constant k_1 whereas the opposite reaction direction should be much less dependent on the field. We therefore consider k_{-1} as approximately independent of E.

The evaluation of the field factor $w_1(E)$ yields an average pore radius of $\bar{r}_p = 0.35(\pm 0.05)$ nm of the assumed cylindrical pore. The value is of the same order as $\bar{r}_p \approx 0.5$ nm derived from conductivity measurements on planar bilayer membranes [9].

The cylinder model yields an estimate of the average cluster size of the lipids in the pore edge. For $\bar{r}_p = 0.35(\pm 0.05)$ nm we obtain $\langle n \rangle = 12(\pm 2)$ lipids per pore edge. For $E > E_{sat}$, the total number of DPH molecules in pore states approaches a saturation value; the fraction of DPH molecules in HI and HI* pores is $12(\pm 2)$% and that in HO and HO* pores is $48(\pm 2)$%. The percentage of membrane area $P \approx (\lambda_m/\lambda_i) \times 100\%$ of conductive openings filled with the intravesicular medium of conductance $\lambda_i = 2.2$ S m^{-1} linearly increases from $P \approx 0\%$ ($E = 1.8$ MV m^{-1}) to $P = 0.017\%$ ($E = 8.5$ MV m^{-1}). Analogous estimations made by Kinosita et al. [15] on the basis of fluorescence imaging data for sea urchin eggs give the same order of magnitude of P (0.02–0.2%). The increase in P with the field strength is collinear with the increase in the concentrations of HI and HI* states with the field strength, whereas the HO and HO* states exhibit a sigmoid field dependence. Therefore our data suggest that it is only the HI and HI* pore states which are conductive. For $E > E_{sat}$, the transient additional contributions to the negative dichroism due to the direct transitions C($\rightleftarrows$ HO*) $\rightleftarrows$ HI$_Q^*$ within the first 6 μs reflect a transiently larger number of conductive pores at an initial membrane voltage $\Delta\varphi_Q \approx 2\Delta\varphi_{sat}$. The negative dichroism suggests that first one of the two pole cap regions becomes more conductive than the other one (in line with Kinosita's et al. [15] fluorescence observations made for sea urchin eggs), such that the other pole cap transiently experiences a membrane voltage twice as large as the stationary value $\Delta\varphi_{sat}$. The quantitative description of the transient feature involves the time constant (τ_{pol}) of the very rapid interfacial polarization of the vesicle and a time dependent distribution constant $K_Q(t, \theta)$, in addition to the time constant of the slower pore closure (τ_{cl}) due to increasing membrane conductivity λ_m^Q of that pole cap region where initially $\Delta\varphi_Q(t \rightarrow 0) = 2\Delta\varphi_{sat}$. Again, the stationary value $\Delta\varphi_{sat}$ is practically independent of E and the number and

size of the pores approaches saturation values for $E > E_{sat}$.

Finally, it is noted that the various peculiar features of the DPH dichroism (and also of the turbidity dichroism of vesicles without the probe DPH) cannot be described by simple deformation of the vesicle. Besides that, in the time range of the pulse duration of only 10 μs, vesicles of size $\varnothing = 400$ nm are not expected to show field-induced deformation (deformation time constant $\tau_{def} > 10$ ms [16]). Therefore, only the chemical phase transition model, describing electroporation in terms of clusters of lipid molecules in the pore edges, is adequate to cover all the experimental observations.

Acknowledgements

We thank the Deutsche Akademische Austauschdienst (DAAD) for a scholarship to S. Kakorin and the Deutsche Forschungsgemeinschaft for a grant to E. Neumann, DFG-Ne 227/9-2.

References

[1] E. Neumann, A.E. Sowers and C.A. Jordan (Eds.), Electroporation and Electrofusion in Cell Biology, Plenum Press, New York, 1989, p. 426.

[2] E. Neumann, M. Schaefer-Ridder, Y. Wang and P.H. Hofschneider, EMBO J., 1 (1982) 841–845.

[3] E. Neumann, Bioelectrochem. Bioenerg., 28 (1992) 247–267.

[4] Y. Mouneimne, P.F. Tosi, Y. Gazitt and C. Nicolau, Biochem. Biophys. Res. Commun., 159 (1989) 34–40.

[5] Y.A. Chizmadzhev, V. Zarnytsin, J.C. Weaver and R.O. Potts, Biophys. J., 68 (1995) 749–765.

[6] J. Belehradek Jr., S. Orlowski, L.H. Ramierez, G. Pron, B. Poddevin and L.M. Mir, Biochim. Biophys. Acta, 1190 (1994) 155–163.

[7] R. Heller and R. Gilbert, Proc. BES Symposium, Bielefeld University Press, 1993, p. 10.

[8] I.G. Abidor, V.B. Arakelyan, L.V. Chernomordik, Y.A. Chizmadzhev, V.F. Pastuchenko and M.R. Tarasevich, Bioelectrochem. Bioenerg., 6 (1979) 37–52.

[9] R.W. Glaser, S.L. Leikin, L.V. Chernomordik, V.F. Pastushenko and I. Sokirko, Biochim. Biophys. Acta, 940 (1988) 275–287.

[10] J.D. Litster, Phys. Lett., 53A (1975) 193–194.

[11] E. Neumann, E. Werner, A. Sprafke and K. Krüger, in B.R. Jennings and S.P. Stoilov (Eds.), Colloid and Molecular Electrooptics, IOP Publishers, Bristol, 1992, pp. 197–206.

[12] M. Spassova, I. Tsoneva, A.G. Petrov, J.I. Petkova and E. Neumann, Biophys. Chem., 52 (1994) 267–274.

[13] A. Revzin and E. Neumann, Biophys. Chem., 2 (1974) 144–150.

[14] G. Schwarz, J. Phys. Chem., 71 (1967) 4021–4030.

[15] M. Habino, H. Itoh and K. Kinosita, Jr., Biophys. J., 64 (1993) 1789–1800.

[16] A. Socirko, V. Pastuchenko, S. Svetina and B. Zeks, Bioelectrochem. Bioenerg., 34 (1994) 101–107.